

Thermal Properties and Characterization of n-Decyl-Lauryl Alcohol/Expanded Graphite/Silicon Carbide Composite Phase Change Materials for Refrigerator Cold Energy Storage

Yanghua CHEN *, Piaopiao HUANG, Xue YANG

College of Mechatronics Engineering, Nanchang University, Nanchang 330031, No.999 Xuefu Road, Honggutan New District, Nanchang City, Jiangxi Province, China

crossref <http://dx.doi.org/10.5755/j02.ms.29758>

Received 07 September 2021; accepted 21 February 2022

In this study, a kind of phase change materials (PCMs) with a low melting point (around 0 °C) was prepared using n-decyl alcohol (DA) and lauryl alcohol (LA) as PCM, expanded graphite (EG) as supporting matrix. Nano silicon carbide (SiC) as a thermal conductivity promoter was added to modify the composite PCM. Expanded graphite with strong adsorption performance was used to not only prevent the leakage, but enhance the thermal conductivity. Leakage experiments showed that the maximum adsorption rate of DA-LA in composite PCM was 92 wt.%. The physical properties and chemical compatibility of composite PCM were studied, and the results showed that the raw materials were well absorbed and dispersed homogeneously into the porous structure of the EG, and they were only a physical bond with each other without chemical reaction. The melting and solidification temperature of composite PCM with the SiC mass ratio 3 wt.% was -0.85 °C and 1.08 °C, and the latent heat of melting and solidification was 85.62 J/g and 74.94 J/g, respectively. The thermal conductivity of composite PCM with 9 wt.% SiC addition was 1.61, which was more than 4.19 times that of pure DA-LA. Thermogravimetric Analysis (TGA) experiment showed that composite PCM had outstanding thermal stability and durability. The present study confirms that this composite PCM is a potential candidate for cold energy storage in refrigerator applications.

Keywords: phase change materials, n-Decyl-Lauryl alcohol, nano-SiC, expanded graphite, cold energy storage, thermal properties.

1. INTRODUCTION

With the rapid development of modernization and the improvement of people's living standards, the demand for energy and the consumption of electricity are increasing by the day. Therefore, it is increasingly important to find a feasible energy saving solution [1]. In the household appliances, the refrigerator as a 24-hour continuous operation of household appliances, has become the highest energy consumption of electrical appliances [2]. According to statistics, China produces more than 80 million refrigerators each year, with a population of about 300 million, and its energy consumption accounts for about 40–50 % of residential electricity consumption [3]. The research on refrigerator energy-saving technology is of great significance to alleviate energy shortages, reduce environmental problems, and realize the sustainable development of the national economy.

Phase change materials (PCMs) are materials that are able to store or release heat energy in the process of phase change at an almost constant temperature. Many researchers have applied PCMs to refrigerators. Angelo et al. used water as the PCM, and put 15.6 kg of tap water on the bare tube evaporator. The results showed that the introduction of PCM reduced the fluctuation of product temperature during the operation of the refrigerator and the temperature difference between the top and the bottom of the refrigerator, and prolonged the OFF time of the compressor [4]. Khan et al.

experimentally studied the use of PCMs behind the five sides of the evaporator. The experimental results indicated that the number of ON-OFF cycles of the compressor was 3–5 times lower than that of the system without PCMs, and the running time was reduced by about 5–30 % [5]. Pirvaram et al. used polyethylene glycol-1000 and polyethylene glycol-600, which were arranged in a cascade configuration, as PCMs, and placed them on the back of the wire-and-tube condenser in the order of their melting temperature decreasing in the direction of refrigerant flow. With results showing that, compared with the refrigerator without PCM, the working time of the compressor and the temperature fluctuation inside the refrigerator were greatly reduced, and the energy consumption was reduced by 13 % [6]. Cheng et al. proposed a regenerative condenser wrapped with the heat conduction enhanced shape-stabilized PCM (HSE-SSPCM), which was made of paraffin, high-density polyethylene and EG. The thermal conductivity of HCE-SSPCM was 1.35 W/m-K, which was 4 times higher than that of traditional PCMs. The new system could significantly improve the overall heat transfer of the refrigeration system [7]. Sonnenrein et al. used copolymer PCMs to apply them to the evaporator and condenser of the refrigerator freezer compartment. They found that the overall power consumption of the refrigerator was reduced by 17 % and the temperature fluctuation of the refrigerator compartment was reduced from 4 °C to 0.5 °C [8]. Gin et al.

* Corresponding author. Tel.: +86-13970944938.
E-mail address: chenyh@ncu.edu.cn (Y. Chen)

[9] placed a PCM aluminum plate with a thickness of 10 mm on the wall of the freezer. It was found that the temperature fluctuation in the freezer was significantly reduced, and it can still be kept at a lower temperature in case of power failure. In another study [10], they found that the energy consumption during refrigerator door opening and defrosting can be reduced by 7 % and 8 % respectively by using PCMs in the freezer compared with that without using PCMs. Elarem et al. put the PCM on the evaporator, walls and racks of the compartment of the refrigerator, which can effectively help to rapidly stabilize and homogenize the temperature, and increase the OFF time of the compressor to achieve the effect of energy saving [11].

Among the PCMs for refrigerators, solid-liquid organic PCMs have become the focus of research due to their chemical and thermal stability, high latent heat, non-toxicity, low subcooling, low cost and corrosion resistance [12, 13]. However, the low thermal conductivity of organic PCMs greatly limits its application. It has been proved that the thermal conductivity of organic PCMs can be effectively improved by adding nanoparticles [14–16] and enhancing the adsorption of heat-conducting porous media [17–19]. Safira et al. prepared a composite PCM that used coconut oil as PCM and sonicating graphene as thermal conductivity enhancer. Through the test found that, when the addition amount of sonicating graphene was 0.3 wt.%, its thermal conductivity was increased by 69% compared with pure PCM [20]. Lin et al. prepared the palmitic acid (PA)/nano-silica composite PCM with the optimum mass ratio of 70:30, the latent heat of melting (H_m) and the melting temperature (T_m) were 128.42 J/g and 60 °C, respectively. Graphene nanosheets were used as a thermal conductivity enhancer. When the mass fraction was 5 wt.%, its thermal conductivity was increased by 1.65 times [21]. Zhang et al. prepared the n-eicosane/nano-silica composite PCM with the best mass ratio of 70:30, the H_m and T_m was 135.8 J/g and 35.35 °C, respectively. EG was used as the thermal conductivity promoter. When the mass fraction of EG was 7 %, the thermal conductivity of the composite PCM was 2.37 times that of the composite PCM without EG [22]. Zhao et al. prepared 1-dodecanol-tetradecane/EG composite PCMs by high-speed emulsification and natural physical adsorption. The T_m and H_m were 3.63 °C and 197.95 J/g, respectively. The best mass ratio of EG was 7 %. Compared with pure PCMs, the thermal conductivity of composite PCMs with EG increased by 10 times [23]. Chi et al. used EG as the porous carrier and graphene oxide (GO) as the surface coating to prepare new myristyl alcohol (MA)/EG-GO composite PCM. Compared with the pure PCM, its thermal conductivity increased by 10.8 times, with good application potential for thermal energy storage [24].

With the continuous development of refrigerator technology, the intermediate thermostatic preservation chamber in the three-door refrigerator can keep food fresh without icing, and preserve the nutrition of the food to the greatest extent without destroying the nutritional structure of the food itself. Although there are many technologies for food preservation in refrigerators, such as precise temperature control, zero-degree vacuum preservation and biological preservation, etc., there is still serious problem in the refrigerator compartment, that is, large temperature fluctuations. This has a vital impact on the quality of food

storage. In the existing research, there are few low-temperature organic PCMs with a temperature range of 0–8 °C, especially for the popular intermediate thermostatic fresh-keeping chamber, and there are almost no scholars to study the low-temperature PCM near 0 °C. Aiming at this temperature range, this study adopts the eutectic method to prepare a new type of n-decyl alcohol (DA)-lauryl alcohol (LA) composite PCM through theoretical predictions and experiments, and uses EG as a support material for adsorption to prevent leakage and improve its thermal conductivity rate. On this basis, nano-SiC is used to further modify the DA-LA/EG composite PCM to improve its thermal conductivity. DA-LA/EG/SiC composite PCM has good phase change enthalpy, high thermal conductivity, and good stability. It has a certain reference value when applied in the theoretical preservation chamber of the refrigerator.

2. MATERIALS AND METHODS

2.1. Materials

Lauryl alcohol ($C_{12}H_{25}OH$, purity > 98 %) and n-decyl alcohol ($C_{10}H_{21}OH$, purity > 98 %) were purchased from Aladdin Biochemical Technology Co., Ltd (Shanghai, China). Nano-SiC (< 300 nm) was obtained from Cote New Materials Technology Co., Ltd. Absolute ethyl alcohol (C_2H_5OH , purity > 99.7 %) was obtained from Xilong Scientific Co., Ltd (Shantou, China). Expanded graphite (C, 80 mesh) was purchased from Tengshengda Graphite Co., Ltd (Qingdao, China). All reagents were analytically pure and can be used directly without treatment.

2.2. Preparation of DA-LA composite PCMs

The theoretical prediction method is used for the preparation of the DA-LA binary eutectic mixture PCMs for minimizing the number of test samples as well as the cost associated with the characterization. The theoretical mass ratios of binary fatty alcohol eutectic mixture are determined by the phase diagram. The Schroeder equation is derived from the second law of thermodynamics and the phase equilibrium theory [25–27]. Schrader equation is presented below:

$$T_M = \left[\frac{1}{T_i} - \frac{R \ln X_i}{H_i} \right]^{-1}, \quad (1)$$

where T_m is the phase change temperature of the DA-LA eutectic mixture; T_i and H_i are the phase change temperature and latent heat of DA and LA, respectively. X_i is the molar ratio of DA (X_1) or LA (X_2), $X_1 + X_2 = 1$. The results from the Schrader equation of the eutectic mixture mass ratio and eutectic melting temperature of the DA-LA curve were shown in Fig. 1. Based on the above theoretical prediction results, a certain quality of DA and LA were weighed with a mass ratio of 75.27:24.73 and put into a 100 ml beaker, then heated in a constant temperature water bath at 40 °C. When the two fatty alcohols were completely melted, stirred them in a magnetic stirrer at 300 r/min for 20 minutes, to ensure that DA and LA can be fully mixed. The mixture was cooled to room temperature to obtain a DA-LA binary eutectic mixture.

2.3. Preparation of DA-LA/EG and DA-LA/EG/SiC composite PCMs

DA-LA/EG and DA-LA/EG/SiC composite PCMs were prepared by melt blending method and vacuum adsorption method.

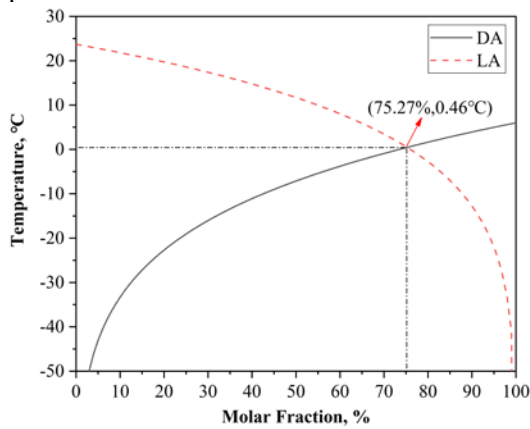


Fig. 1. The predicted phase diagram of the DA-LA binary eutectics

Firstly, a certain mass of EG was put into a 500 ml beaker, and placed in a vacuum drying oven at 70 °C for 12 hours to dry the water in it to obtain usable expanded graphite. Then, a certain mass of DA-LA mixture in a beaker was put into a constant temperature water bath at a temperature of 40 °C, and slowly pour EG with a mass ratio of 5 % into the beaker for mechanical stirring for 1 hour. The same method was used for EG with other mass percentages. Finally, it was put into a vacuum drying oven at a temperature of 70 °C for vacuum adsorption for 12 hours, DA-LA/EG composite PCMs were obtained.

The production method of DA-LA/EG/SiC is similar to that of DA-LA/EG, just add a certain quality of SiC to the beaker before adding EG, and stir for 20 minutes to ensure that SiC is fully dispersed in the DA-LA solution. As a result, DA-LA/EG/SiC composite PCMs with different mass ratios were prepared (the ratios were 3 %, 5 %, 7 % and 9 %). The experimental flowchart is shown in Fig. 2.

2.4. Characterization

The chemical structural analysis of the EG and

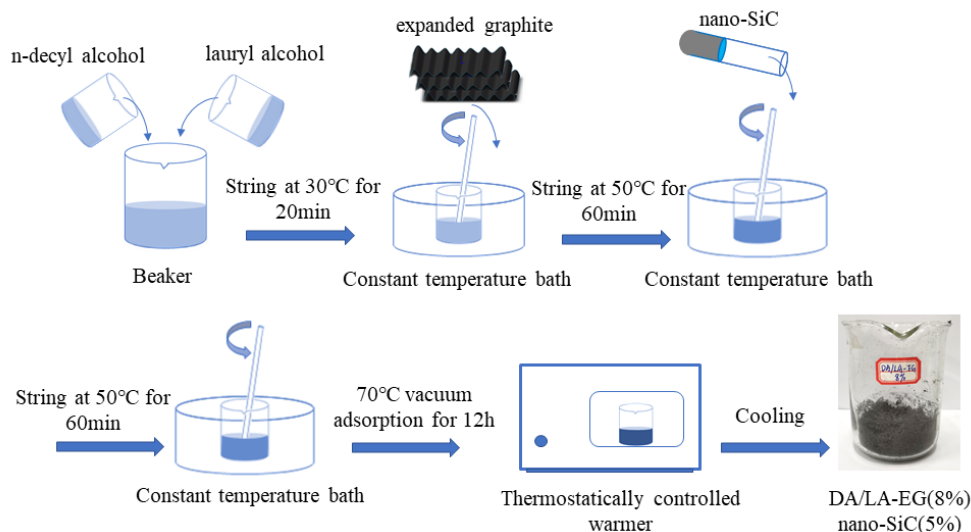


Fig. 2. The processing sketch for preparation of the composite PCMs

composite PCMs was carried out by Fourier Transform Infrared Spectroscopy (FT-IR) spectrophotometer (Nicolet iS50) using KBr pellet at the frequency range of 4000 cm^{-1} to 400 cm^{-1} . In the nitrogen atmosphere and the heating rate was 10 °C/min in the temperature range of -20 °C to 80 °C. The surface morphologies and microstructures of raw EG and composite PCMs were analyzed by Quanta200 FEG environmental scanning electron microscope (ESEM). The ESEM images were taken with high resolution and 20 kV acceleration voltage in low vacuum mode. Differential Scanning Calorimeter (DSC, 8000, PerkinElmer, USA) was used to investigate the thermal energy storage properties of the DA-LA and composite PCMs. In this process, all samples were heated and cooled repeatedly between -20 °C and 30 °C and heating-cooling rate of 5 °C/min under a constant stream of nitrogen at a flow rate of 10 ml/min. The thermal conductivity of different composite PCMs was analyzed by Thermal Conductivity Meter (Hot Disk) (TPS 2500 s) at 25 °C. Among them, the sample was compressed into two cylinders with a diameter of 25 mm and a thickness of 5 mm. Put a polyimide-coated probe (5501, $R = 6.403 \text{ mm}$) in the middle of the two cylinders to measure the thermal conductivity. Each sample was tested 3 times. Thermogravimetric Analysis (TGA) was used to study the weight change of composite PCMs with temperature. The measurements were conducted by heating the samples from 30 °C to 600 °C at a heating rate of 10 °C/min under nitrogen atmosphere with a flow rate of 20 ml/min.

3. RESULTS AND DISCUSSION

3.1. Determination of the optimum mass ratio of DA-LA to EG

When PCMs are applied in the field of a household refrigerator, the leakage of PCMs will contaminate food in the refrigerator and cause harm to the human body to a certain extent. Therefore, it is very important to prevent the leakage of PCMs. Due to its porous structure, EG can effectively adsorbate DA-LA and improve its thermal conductivity.

Although excessive EG will not affect the phase change temperature of DA-LA, it will affect the latent heat value of DA-LA, which is very important for the application of PCM [19]. Therefore, it is of great significance to determine the optimal mass ratio of DA-LA. In the experiment, 0.5 g molten state samples were weighed and placed on the filter paper and placed in the drying oven with a temperature of 50 °C for static treatment. The weighing results were carried out every half an hour, as shown in Fig. 3.

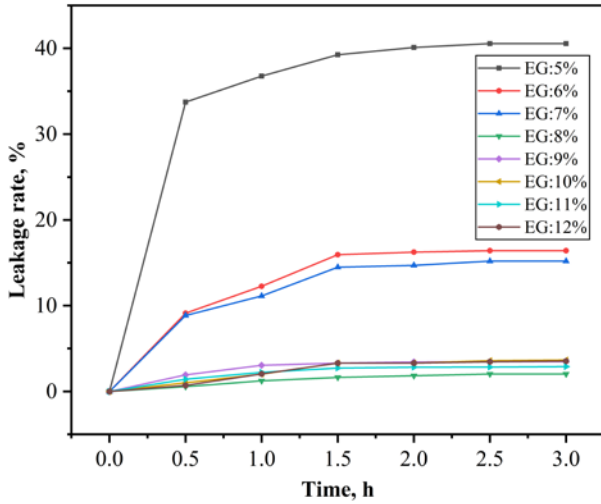


Fig. 3. Leakage rate of different DA-LA/EG samples

Table 1 lists the mass loss and percentage change of mass loss before and after weighing. It can be clearly seen from the figure that with the increase of EG content, the leakage rate of DA-LA/EG gradually decreased. Among them, when the content of EG was 5 %, the leakage rate reached 40.56 %. This was because the content of DA-LA greatly exceeded the adsorption capacity of EG, and the excess liquid DA-LA was absorbed by the filter paper after leakage. When the mass ratio of EG exceeded 8 %, the mass loss ratio of DA-LA in the composite phase change material was less than 4 %, which may be caused by measurement and observation errors [28]. Based on the above results, it was determined that the best mass percentage of EG in DA-LA was 8 %. Therefore, in the following research, DA-LA/EG-8 composite phase change material was the object of continued research.

3.2. FT-IR analysis

To characterize the chemical compatibility among components, Fig. 4 shows the FT-IR spectra of EG, SiC, DA-LA, DA-LA/EG and DA-LA/EG/SiC-7%. The

absorption at 3340 cm^{-1} , which was very strong and broad, was attributed to the stretching vibration of the -OH group. The peaks at 2962 cm^{-1} , 2927 cm^{-1} and 2856 cm^{-1} belong to the C-H bond stretching vibration of the -CH₃ and -CH₂ groups, respectively [23]. However, the peaks of 1461 cm^{-1} and 1378 cm^{-1} represented the scissor bending vibration of the -CH₂ functional group and the in-plane bending vibration of the -CH₃ functional group [25]. There was an absorption peak at 1059 cm^{-1} , which was characterized by the asymmetric stretching vibrations of the -C-O functional group. The peak at 721 cm^{-1} denoted the in-plane rocking vibration of the -CH₂ group.

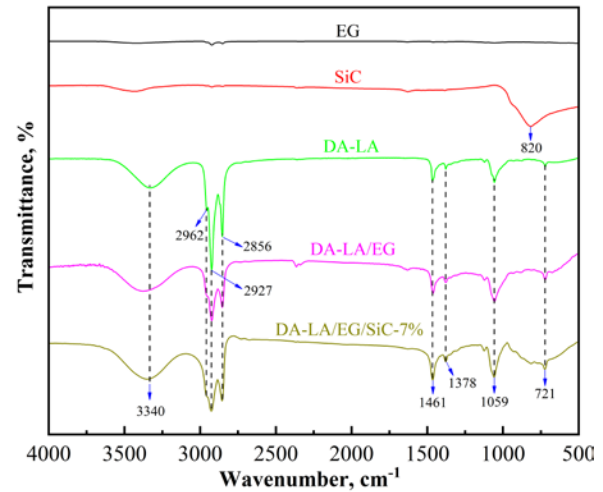


Fig. 4. FT-IR spectra of the EG, SiC, DA-LA, DA-LA/EG and DA-LA/EG/SiC-7% composite PCM

EG, which was composed of the carbon element, had no absorption peak in FT-IR spectra. In the SiC spectrum, there was a wide absorption peak at 820 cm^{-1} , which was due to the stretching vibration of Si-C bond [29]. Conclusively, all the characteristic absorption peaks in DA-LA existed simultaneously in the spectra of DA-LA/EG and DA-LA/EG/SiC. There was no new absorption peak and no peak position move. DA-LA was merely adsorbed by EG in the pores without any chemical reaction but physical adsorption. The result indicated that DA-LA had good compatibility with EG and SiC.

3.3. Morphological analysis

The surface morphologies and microstructures of EG, SiC and DA-LA/EG/SiC composite PCMs were observed by ESEM at different magnification and are shown in Fig. 5.

Table 1. Weight loss of composite PCM samples before and after the thermal treatment

Samples	Mass before standing treatment, g	Mass after standing treatment, g	Mass loss, g	Mass loss percentage, %
DA-LA/EG-5	0.5000	0.2972	0.2028	40.56
DA-LA/EG-6	0.5054	0.4224	0.0830	16.42
DA-LA/EG-7	0.5020	0.4257	0.0763	15.20
DA-LA/EG-8	0.5010	0.4908	0.0102	2.04
DA-LA/EG-9	0.5010	0.4836	0.0174	3.47
DA-LA/EG-10	0.5017	0.4833	0.0184	3.66
DA-LA/EG-11	0.5013	0.4868	0.0145	2.89
DA-LA/EG-12	0.5016	0.4838	0.0178	3.54

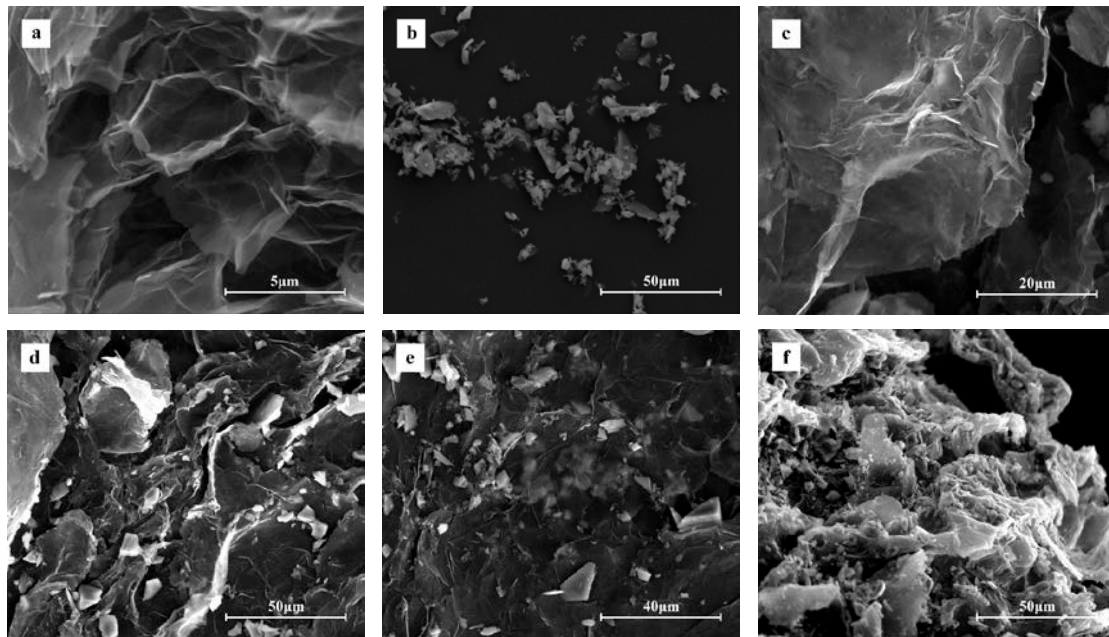


Fig. 5. ESEM photographs: a – EG; b – nano-SiC; c – CPCM-0; d – CPCM-3; e – CPCM-7, f – CPCM-9

The ESEM of EG in Fig. 5 a showed that EG had a porous structure and well-developed network pores can be clearly observed at the micro-scale [30]. This porous structure increased its specific surface area, so that DA-LA in the molten state was more easily adsorbed, and its adsorption rate can reach 92 wt.%. Moreover, due to the capillary force of the porous microstructure in EG, DA-LA was tightly wrapped in its porous structure, as shown in Fig. 5 c, which can effectively prevent the leakage of the loaded DA-LA [31]. After adding nano-SiC to DA-LA/EG, nano-SiC with crystal structure was evenly distributed in the interlaminar and micropore of EG. As can be seen from Fig. 5 e, a part of nano-SiC was wrapped in EG thin layer, which had no regular morphology and no agglomeration. As the mass fraction of nano-SiC increased, the surface of the DA-LA/EG become rougher. This was because a large amount of nano-SiC adhered to the surface of EG, increasing the contact area with DA-LA, and enhancing the thermal conductivity of the composite PCMs. Consequently, the addition of nano-SiC had a good supporting effect on DA-LA/EG, which can further prevent the leakage of DA-LA.

3.4. Thermal properties analysis

The thermostatic chamber in the three-door refrigerator has strict requirements for temperature control. Therefore, the T_m and T_s within the working range are one of the key

parameters for considering the corresponding PCMs. Other thermal properties include excellent H_m and H_s , which indicate better energy storing/releasing PCM performances with a smaller mass and volume, and its cost-effective [23]. The thermal properties of DA-LA, CPCM-0, CPCM-3, CPCM-5, CPCM-7 and CPCM-9 were measured via DSC. The relevant data are listed in Table 2, and the phase transition process is shown in Fig. 6. All DSC curves of CPCMs were operated under the first heating/cooling. It can be seen from the table that the melting and solidification temperatures of DA-LA were -1.25°C and 0.72°C , respectively, and the corresponding latent heats of melting and solidification were 113.92 J/g and 96.71 J/g , respectively. The melting and solidification temperatures of CPCM-0, CPCM-3, CPCM-5, CPCM-7 and CPCM-9 are $-0.77/1.33^\circ\text{C}$, $-0.85/1.08^\circ\text{C}$, $-0.77/1.39^\circ\text{C}$, $0.12/2.23^\circ\text{C}$ and $0.13/2.24^\circ\text{C}$, respectively. Compared with pure DA-LA, due to the addition of EG, its microporous structure limited the melting and solidification process of DA-LA, which increased the melting point and freezing point temperature of CPCM, but its phase change temperature still met the requirements of PCMs near 0°C used in the thermostatic chamber of the refrigerator. It was worth noting that the peaks of CPCM and DA-LA were similar, which stated clearly that the phase transformation behavior of CPCM and DA-LA was similar, further indicating that the addition of EG and SIC had no effect on the thermal properties of DA-LA.

Table 2. The thermal properties of the PCMs during melting and solidification

Samples	Melting			Solidifying		
	Onset temperature, $^\circ\text{C}$	Peak temperature, $^\circ\text{C}$	Latent heat, J/g	Onset temperature, $^\circ\text{C}$	Peak temperature, $^\circ\text{C}$	Latent heat, J/g
DA-LA	-1.25	2.6	113.92	0.72	-3.56	96.71
CPCM-0	-0.77	2.01	94.69	1.33	-1.54	81.06
CPCM-3	-0.85	1.86	85.62	1.08	-2.87	74.94
CPCM-5	-0.77	1.81	71.98	1.39	-1.25	69.22
CPCM-7	0.12	3.51	70.05	2.23	-1.30	75.56
CPCM-9	0.13	3.51	69.79	2.24	-1.30	66.55

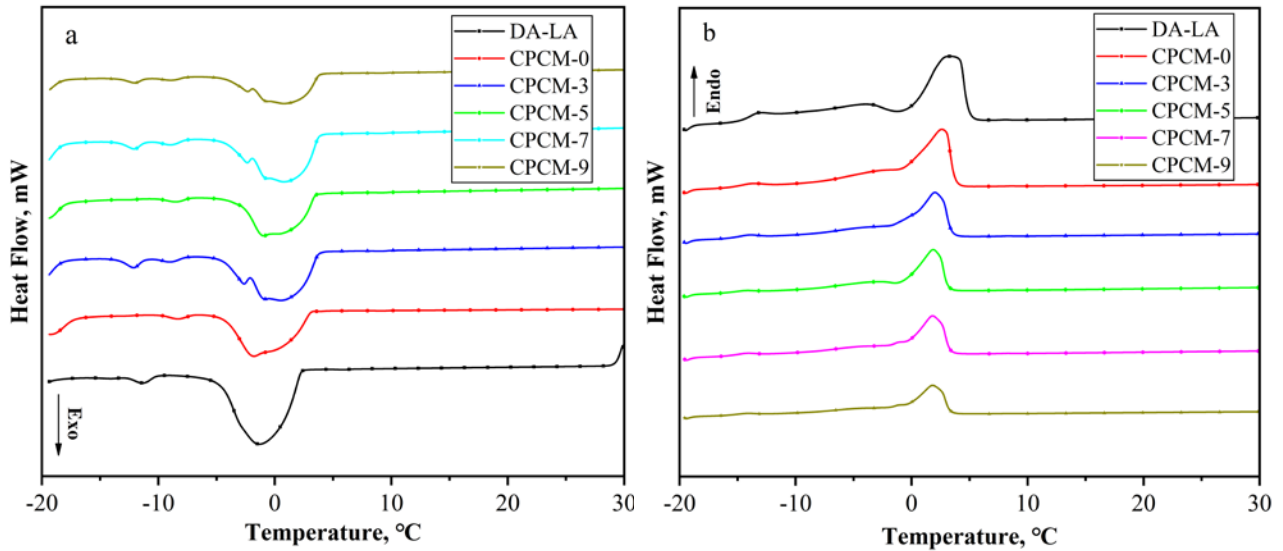


Fig. 6. a – solidifying DSC curves; b – melting DSC curves of DA-LA and CPCMs

The latent heat of melting and solidification of CPCM-0, CPCM-3, CPCM-5, CPCM-7 and CPCM-9 were 94.69/81.06 J/g, 85.62/74.94 J/g, 71.98/69.22 J/g, 70.05/75.56 J/g and 69.79/66.55 J/g, respectively. Obviously, the latent heat of CPCMs decreases with the increase of SiC, because the latent heat in CPCM was only related to the ratio of DA-LA. Therefore, the theoretical latent heat values can be calculated by the following formula:

$$\Delta H_{theoretical} = \Delta H_{DA-LA} \times (w_{EG/SiC}\%), \quad (2)$$

where $\Delta H_{theoretical}$ represents the theoretical value of CPCM; ΔH_{DA-LA} represents the latent heat of DA-LA; and $w_{EG/SiC}$ is the EG/SiC mass fraction in the CPCM. It had been calculated that the experimental test value of CPCM was lower than the theoretical value. One was due to the abnormal interaction between PCM and the inner surface of EG pores, the other was due to the testing error of DSC [32]. In conclusion, the DA-LA/EG/SiC PCMs with suitable phase change temperature and higher latent heat was a better choice for refrigerator 0 °C thermostatic chamber applications.

3.5. Thermal conductivity

The thermal conductivity of PCMs is one of the important parameters for low-temperature thermal energy storage applications, because it significantly affects the rate of heat storage and release [28]. In this work, the thermal conductivity of DA-LA, DA-LA/EG and DA-LA/EG/SiC composite PCMs was measured by the Hot Desk. The test conditions were carried out at an ambient temperature of 20 °C. As shown in Fig. 7, the thermal conductivity of DA-LA was about 0.31 W/m·K, which was too low for thermal energy storage to meet the requirements. The thermal conductivity of DA-LA/EG rapidly increased to 1.13 W/m·K by adding 8 % of EG. Compared with pure DA-LA, the thermal conductivity is increased by 265 %. To further improve the thermal conductivity of CPCM, SiC modified particles were added to DA-LA/EG. It can be seen

from Fig. 7 that the thermal conductivity of CPCM increased with the increase of the mass fraction of SiC. When it was 3 wt.%, the thermal conductivity of CPCM reached 1.31 W/m·K.

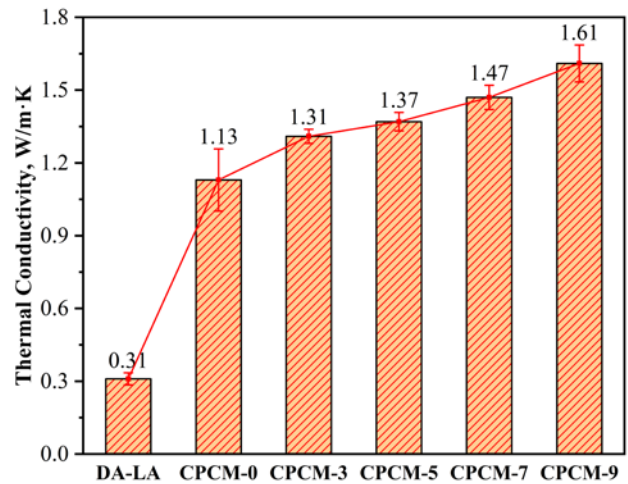


Fig. 7. The thermal conductivity of pure DA-LA and the prepared CPCMs

When it was 9 wt.%, the thermal conductivity of CPCM reached 1.61 W/m·K. Compared with the thermal conductivity with only EG added, the thermal conductivity was increased by 42.5 %, and the thermal conductivity was increased by 419 % compared with pure DA-LA. On the one hand, SiC itself was a kind of high thermal conductivity particle, and on the other hand, SiC was filled in the EG honeycomb pores, supporting the EG skeleton structure so that the thermal conductivity of EG maintains good continuity and integrity, and enhanced its thermal conductivity. Therefore, SiC was an effective thermal conductivity additive for composite PCMs. However, with the increase of SiC mass fraction, the thermal conductivity of CPCM will increase accordingly, but too much SiC will reduce the mass proportion of DA-LA in CPCM, resulting in a decrease in the latent heat in CPCM.

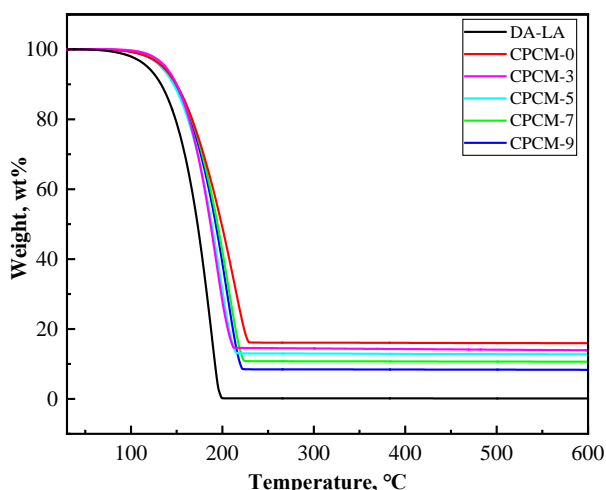
Table 3. Characteristic temperatures and charred residue at 600°C of the DA-LA and DA-LA/EG/SiC composite PCMs

Samples	Mass of DA-LA, g	Mass of EG, g	Mass of SiC, g	Mass rate of EG/SiC, %	T_{onset} , °C	T_{max} , °C	Charred residue amount, %
DA-LA	18.4	1.6	–	–	82.6	199.9	0.1
CPCM-0	18.4	1.6	–	8.0	105.7	216.4	8.3
CPCM-3	18.4	1.6	0.6	10.7	105.7	222.1	10.6
CPCM-5	18.4	1.6	1.0	12.4	105.7	223.6	12.7
CPCM-7	18.4	1.6	1.4	14.0	105.7	229.8	13.9
CPCM-9	18.4	1.6	1.8	15.6	105.7	214.1	15.9

Hence, we need to pay more attention to improve the thermal conductivity of CPCM and meet the high latent heat at the same time. Combining the phase change latent heat and thermal conductivity of CPCM, CPCM with a mass fraction of SiC of 3 wt.% was the most ideal refrigerator cold energy storage material.

3.6. Thermal stability

TGA was carried out to characterize the influence of EG and SiC on the thermal stability of composite PCMs, which determined the availability and sustainability of PCM [29]. The results of DA-LA and CPCM samples are shown in Fig. 8 and Table 3.

**Fig. 8.** TGA curve of DA-LA and different CPCMs

It can be found that there was a single mass loss process from 30 °C to 600 °C for DA-LA and CPCMs, which was attributed to the vaporization and decomposition of fatty alcohol. As the temperature increased, the onset decomposition temperature (T_{onset}) of DA-LA was 82.6 °C in a nitrogen atmosphere and the maximum mass loss percentage (T_{max}) was almost 100 % at about 199.9 °C. However, the degradation curves of CPCMs were commenced at 105.6 °C and were completed at about 220 °C. According to Fig. 8, the initial degradation temperature of CPCMs was obviously higher than that of pure PCM. The results indicated that EG can effectively slow down the mass loss process and improve the thermal stability of DA-LA, which was due to the use of EG as a support material via van der Waals force [23]. In Table 3, the charred residues of composite PCMs were in good agreement with the loading rate of raw material EG and SiC in the PCM, respectively. Thus, the TGA results suggested

that the composite PCMs had good thermal stability in low-temperature applications.

4. CONCLUSIONS

In this work, DA-LA, with its melting latent heat of 113.92 J/g and melting temperature of -1.25 °C, was chosen as a low-temperature eutectic PCM. EG, with good adsorption, was used as the supporting material. SiC with high thermal conductivity was utilized to modify CPCM thermal conductivity. Leakage experiment results show that the maximum adsorption rate of DA-LA in EG was 92 wt.%, and then 3, 5, 7 and 9 wt.% SiC were, respectively, added to the CPCM in this proportion. The chemical and morphological characterizations were carried out by SEM and FT-IR. The results showed that SiC was successfully adsorbed on the surface and pores of EG, and DA-LA/SiC and EG were only physically combined and no chemical reaction occurred. Its thermal performance was characterized by DSC, TGA and Hot Disk. The analysis results showed that the melting and solidification temperature of CPCM-3 containing 3 wt.% SiC was -0.85 °C and 1.08 °C, and the latent heat of melting and solidification was 85.62 J/g and 74.94 J/g. The TGA results showed that CPCM had good thermal stability and reliability within its phase transition temperature range. SiC effectively improved the thermal conductivity of DA-LA/EG composite PCMs. The thermal conductivity of CPCM-3 was 1.21 times that of DA-LA/EG and 4.23 times that of pure DA-LA. The application of DA-LA/EG/SiC composite PCM in the thermostatic chamber of the refrigerator had suitable phase change temperature, good thermal stability, high thermal conductivity and high energy storage density, which had a very good application prospect.

REFERENCES

1. **Hosseini, S.E., Wahid, M.A.** Hydrogen Production from Renewable and Sustainable Energy Resources: Promising Green Energy Carrier for Clean Development *Renewable and Sustainable Energy Reviews* 57 2016: pp. 850–866. <https://doi.org/10.1016/j.rser.2015.12.112>
2. **Jasmin G., Rainer S.** Analysis of Effecting Factors on Domestic Refrigerators' Energy Consumption in Use *Energy Conversion and Management* 76 2013: pp. 794–800. <https://doi.org/10.1016/j.enconman.2013.08.027>
3. **Cheng, W.I., Ding, M., Yuan, X.D., Han, B.C.** Analysis of Energy Saving Performance for Household Refrigerator with Thermal Storage of Condenser and Evaporator *Energy Conversion and Management* 132 2017: pp. 180–188. <https://doi.org/10.1016/j.enconman.2016.11.029>

4. **Maiorino, A., Del Duca, M.G., Mota-Babiloni, A., Greco, A., Aprea, C.** The Thermal Performances of A Refrigerator Incorporating a Phase Change Material *International Journal of Refrigeration* 100 2019: pp. 255–264.
<https://doi.org/10.1016/j.ijrefrig.2019.02.005>
5. **Khan, M.I.H., Afroz, H.M.M.** Effect of Phase Change Material on Compressor On-Off Cycling of a Household Refrigerator *Science And Technology for the Built Environment* 21 (4) 2015: pp. 462–468.
<https://doi.org/10.1080/23744731.2015.1023161>
6. **Pirvaram, A., Sadrameli, S.M., Abdolmaleki, L.** Energy Management of A Household Refrigerator Using Eutectic Environmental Friendly Pcms in A Cascaded Condition *Energy* 181 2019: pp. 321–330.
<https://doi.org/10.1016/j.energy.2019.05.129>
7. **Cheng, W.L., Mei, B.J., Liu, Y.N., Huang, Y.H., Yuan, X.D.** A Novel Household Refrigerator with Shape-Stabilized PCM (Phase Change Material) Heat Storage Condensers: An Experimental Investigation *Energy* 36 (10) 2011: pp. 5797–5804.
<https://doi.org/10.1016/j.energy.2011.08.050>
8. **Sonnenrein, G., Baumhögger, E., Elsner, A., Fieback, K., Morbach, A., Paul, A., Vrabec, J.** Copolymer-Bound Phase Change Materials for Household Refrigerating Appliances: Experimental Investigation of Power Consumption, Temperature Distribution and Demand Side Management Potential *International Journal of Refrigeration* 60 2015: pp. 166–173.
<https://doi.org/10.1016/j.ijrefrig.2015.06.030>
9. **Gin, B., Farid, M.M.** The Use of PCM Panels to Improve Storage Condition of Frozen Food *Journal of Food Engineering* 100 (2) 2010: pp. 372–376.
<https://doi.org/10.1016/j.jfoodeng.2010.04.016>
10. **Gin, B., Farid, M.M., Bansal, P.K.** Effect of Door Opening and Defrost Cycle on A Freezer with Phase Change Panels *Energy Conversion and Management* 51 (12) 2010: pp. 2698–2706.
<https://doi.org/10.1016/j.enconman.2010.06.005>
11. **Elarem, R., Mellouli, S., Abhilash, E., Jemni, A.** Performance Analysis of A Household Refrigerator Integrating A PCM Heat Exchanger *Applied Thermal Engineering* 125 2017: pp. 1320–1333.
<https://doi.org/10.1016/j.applthermaleng.2017.07.113>
12. **Magendran, S. S., Khan, F.S.A., Mubarak, N.M., Vaka, M., Walvekar, R., Khalid, M., Abdullah, E.C., Nizamuddin, S., Karri, R.R.** Synthesis of Organic Phase Change Materials (PCM) for Energy Storage Applications: A Review *Nano-Structures & Nano-Objects* 20 2019: pp. 100399.
<https://doi.org/10.1016/j.nanoso.2019.100399>
13. **Zhao, Y., Zhang, X., Hua, W.** Review of Preparation Technologies of Organic Composite Phase Change Materials in Energy Storage *Journal of Molecular Liquids* 336 2021: pp. 115923.
<https://doi.org/10.1016/j.molliq.2021.115923>
14. **Yuan, Y., Zhang, N., Li, T., Cao, X., Long, W.** Thermal Performance Enhancement of Palmitic-Stearic Acid by Adding Graphene Nanoplatelets and Expanded Graphite for Thermal Energy Storage: A Comparative Study *Energy* 97 2016: pp. 488–497.
<https://doi.org/10.1016/j.energy.2015.12.115>
15. **Sharma, R.K., Ganesan, P., Tyagi, V.V., Metselaar, H.S.C., Sandaran, S.C.** Thermal Properties and Heat Storage Analysis of Palmitic Acid-Tio 2 Composite as Nano-Enhanced Organic Phase Change Material (NEOPCM) *Applied Thermal Engineering* 99 2016: pp. 1254–1262.
<https://doi.org/10.1016/j.applthermaleng.2016.01.130>
16. **Sarı, A., Bicer, A., Al-Ahmed, A., Al-Sulaiman, F.A., Zahir, M.H., Mohamed, S.A.** Silica Fume/Capric Acid-Palmitic Acid Composite Phase Change Material Doped with Cnts For Thermal Energy Storage *Solar Energy Materials and Solar Cells* 179 2018: pp. 353–361.
<https://doi.org/10.1016/j.solmat.2017.12.036>
17. **Yang, Z., Deng, Y., Li, J.** Preparation of Porous Carbonized Woods Impregnated with Lauric Acid as Shape-Stable Composite Phase Change Materials *Applied Thermal Engineering* 150 2019: pp. 967–976.
<https://doi.org/10.1016/j.applthermaleng.2019.01.063>
18. **Wan, X., Su, L., Guo, B.** Design and Preparation of Novel Shapeable PEG/Sio2/AA Shape-Stabilized Phase Change Materials Based on Double-Locked Network with Enhanced Heat Storage Capacity for Thermal Energy Regulation and Storage *Powder Technology* 353 2019: pp. 98–109.
<https://doi.org/10.1016/j.powtec.2019.03.045>
19. **Zhang, H., Gao, X., Chen, C., Xu, T., Fang, Y., Zhang, Z.** A Capric–Palmitic–Stearic Acid Ternary Eutectic Mixture/Expanded Graphite Composite Phase Change Material for Thermal Energy Storage *Composites Part A: Applied Science and Manufacturing* 87 2016: pp. 138–145.
<https://doi.org/10.1016/j.compositesa.2016.04.024>
20. **Safira, L., Putra, N., Trisnadewi, T., Kusrini, E., Mahlia, T.M.I.** Thermal Properties of Sonicated Graphene in Coconut Oil as A Phase Change Material for Energy Storage in Building Applications *International Journal of Low-Carbon Technologies* 15 (4) 2020: pp. 629–636.
<https://doi.org/10.1093/ijlct/ctaa018>
21. **Lin, Y., Cong, R., Chen, Y., Fang, G.** Thermal Properties and Characterization of Palmitic Acid/Nano Silicon Dioxide/Graphene Nanoplatelet for Thermal Energy Storage *International Journal of Energy Research* 44 (7) 2020: pp. 5621–5633.
<https://doi.org/10.1002/er.5311>
22. **Zhang, X., Zhu, C., Fang, G.** Preparation and Thermal Properties of N-Eicosane/Nano-Sio2/Expanded Graphite Composite Phase-Change Material for Thermal Energy Storage *Materials Chemistry and Physics* 240 2020: pp. 122178.
<https://doi.org/10.1016/j.matchemphys.2019.122178>
23. **Zhao, L., Li, M., Yu, Q., Zhang, Y., Li, G., Huang, Y.** Improving the Thermal Performance of Novel Low-Temperature Phase Change Materials Through the Configuration of 1-Dodecanol-Tetradecane Nanofluids/Expanded Graphite Composites *Journal of Molecular Liquids* 322 2021: pp. 114948.
<https://doi.org/10.1016/j.molliq.2020.114948>
24. **Chi, B., Yao, Y., Cui, S., Jin, X.** Preparation of Graphene Oxide Coated Tetradecanol/Expanded Graphite Composite Phase Change Material for Thermal Energy Storage *Materials Letters* 282 2021: pp. 128666.
<https://doi.org/10.1016/j.matlet.2020.128666>
25. **Liu, Y., Chen, Y.** Preparation and Properties of Lauryl Alcohol-Caprylic Acid Eutectics/Activated Charcoal Composites as Shape-Stabilized Phase Change Materials for Cold Energy Storage *Materials Science (Medžiagotyra)* 26 (3) 2020: pp. 300–307.
<https://doi.org/10.5755/j01.ms.26.3.21371>
26. **Nazir, H., Batool, M., Ali, M., Kannan, A.M.** Fatty Acids Based Eutectic Phase Change System for Thermal Energy

- Storage Applications *Applied Thermal Engineering* 142 2018: pp. 466–475.
<https://doi.org/10.1016/j.applthermaleng.2018.07.025>
27. **Huang, X., Alva, G., Liu, L.K., Fang, G.Y.** Preparation, Characterization And Thermal Properties of Fatty Acid Eutectics/Bentonite/Expanded Graphite Composites as Novel Form Stable Thermal Energy Storage Materials *Solar Energy Materials and Solar Cells* 166 2017: pp. 157–166.
<https://doi.org/10.1016/j.solmat.2017.03.026>
 28. **Yang, X., Yuan, Y., Zhang, N., Cao, X., Liu, C.** Preparation and Properties of Myristic–Palmitic–Stearic Acid/Expanded Graphite Composites as Phase Change Materials for Energy Storage *Solar Energy* 99 2014: pp. 259–266.
<https://doi.org/10.1016/j.solener.2013.11.021>
 29. **Gong, S., Cheng, X., Li, Y., Wang, X., Wang, Y., Zhong, H.** Effect of Nano-Sic On Thermal Properties of Expanded Graphite/1-Octadecanol Composite Materials for Thermal Energy Storage *Powder Technology* 367 2020: pp. 32–39.
<https://doi.org/10.1016/j.powtec.2020.03.039>
 30. **Tang, X., Zhu, B., Xu, M., Zhang, W., Yang, Z., Zhang, Y., Yin, G., He, D., Wei, H., Zhai, X.** Shape-Stabilized Phase Change Materials Based on Fatty Acid Eutectics/Expanded Graphite Composites for Thermal Storage *Energy and Buildings* 109 2015: pp. 353–360.
<https://doi.org/10.1016/j.enbuild.2015.09.074>
 31. **Zhang, N., Yuan, Y., Du, Y., Cao, X., Yuan, Y.** Preparation and Properties of Palmitic–Stearic Acid Eutectic Mixture/Expanded Graphite Composite as Phase Change Material for Energy Storage *Energy* 78 2014: pp. 950–956.
<https://doi.org/10.1016/j.energy.2014.10.092>
 32. **Zhang, N., Yuan, Y., Wang, X., Cao, X., Yang, X., Hu, S.** Preparation and Characterization of Lauric–Myristic–Palmitic Acid Ternary Eutectic Mixtures/Expanded Graphite Composite Phase Change Material for Thermal Energy Storage *Chemical Engineering Journal* 231 2013: pp. 214–219.
<https://doi.org/10.1016/j.cej.2013.07.008>



© Chen et al. 2022 Open Access This article is distributed under the terms of the Creative Commons Attribution 4.0 International License (<http://creativecommons.org/licenses/by/4.0/>), which permits unrestricted use, distribution, and reproduction in any medium, provided you give appropriate credit to the original author(s) and the source, provide a link to the Creative Commons license, and indicate if changes were made.